Journal of Sol-Gel Science and Technology (2019) 91:198–207
https://doi.org/10.1007/s10971-019-04972-x

ORIGINAL PAPER: SOL-GEL AND HYBRID MATERIALS WITH SURFACE MODIFICATION FOR APPLICATIONS

Check for updates

Facile surface modification of ceramic membranes using binary TiO_2/SiO_2 for achieving fouling resistance and photocatalytic degradation

Jongman Lee[1,2] · Jang-Hoon Ha[1] · In-Hyuck Song[1,2] · Jin-Woo Park[3]

Received: 26 August 2018 / Accepted: 14 March 2019 / Published online: 26 March 2019

Abstract

Inorganic surface modification was carried out using a TiO_2/SiO_2 sol–gel process to enhance photocatalytic activity and to mitigate fouling of alumina microfiltration membranes. Pristine alumina membranes were subjected to TiO_2/SiO_2 coating with varied TiO_2 mole percentages. Upon the formation of the TiO_2/SiO_2 layer, small changes in the surface morphology, pore size, and specific surface area were detected. Particularly, as the pore size decreased with the decrease in TiO_2 content, the pure water permeability also gradually diminished. By examining the binary TiO_2/SiO_2 compositions, the optimized conditions demonstrating both higher flux performance and greater photocatalytic activity were determined. Thus, the inorganic surface modification by TiO_2/SiO_2 coating could contribute significantly to the realization of self-cleaning ceramic membranes while extending the membrane cleaning cycle and accelerating productivity.

Graphical Abstract

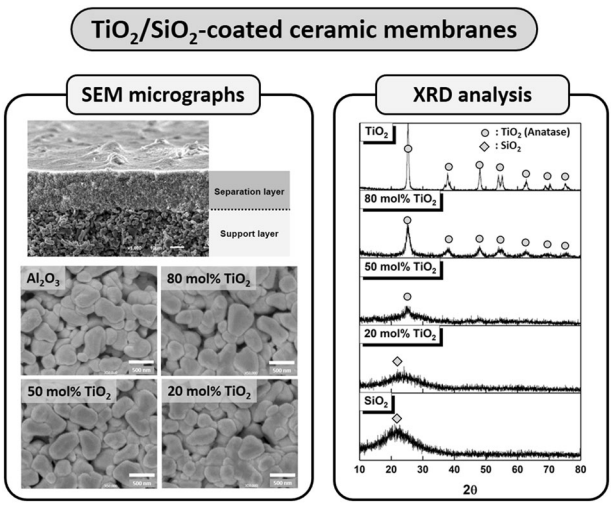

Supplementary information The online version of this article (https://doi.org/10.1007/s10971-019-04972-x) contains supplementary material, which is available to authorized users.

✉ Jongman Lee
jmlee@kims.re.kr

[1] Powder and Ceramics Division, Korea Institute of Materials Science (KIMS), 797 Changwondaero, Seongsangu, Changwon 51508, Republic of Korea

[2] Department of Advanced Materials Engineering, University of Science & Technology (UST), 797 Changwondaero, Seongsangu, Changwon 51508, Republic of Korea

[3] Nano Co., Ltd., 60 Magonggongdanro, Cheongni, Sangju, Gyeongbuk 37257, Republic of Korea

Highlights

- Ceramic microfiltration (MF) membranes are modified using TiO_2/SiO_2 sol–gel process.
- Both fouling resistance and photocatalytic activity are successfully obtained while varying binary TiO_2/SiO_2 compositions.
- The optimized conditions were found at 50 mol% TiO_2 (the second highest flux performance and greater photocatalytic degradation ratio).

Keywords Ceramic membrane · Sol–gel process · Surface modification · Antifouling · Photocatalysis

1 Introduction

Low-pressure ceramic membranes such as microfiltration (MF)/ultrafiltration (UF) membranes have been widely developed for the physical removal of particles of sizes 0.01–10 μm from suspensions [1]. They are usually composed of three layers with different pore structures: support layer, intermediate layer, and thin separation layer [2]. Ceramic membranes have found commercial success in applications in which the operating conditions are harsh, such as at high temperature and in aggressive chemicals (solvent and highly acidic or caustic solutions). Examples of successful commercial-scale applications using ceramic MF/UF membranes include purifying and concentrating valuable components in biotechnology, food, and petrochemical industries [3–5]. In contrast, ceramic membranes are less commonly used in water and wastewater treatment, such as for the production of drinking water and treatment of municipal wastewater. This is mostly ascribed to their high fabrication costs compared with those of polymeric membranes. Nevertheless, the membrane manufacturing technology using low-cost ceramic raw materials has been investigated to offset the use of expensive raw materials and high-temperature sintering processes (>1300 °C) [6, 7]. Membrane materials such as alumina (Al_2O_3) [8], zirconia (ZrO_2) [9], titania (TiO_2) [10], silica (SiO_2) [11], silicon carbide (SiC) [12], and zeolite [13] have been mainly utilized. Moreover, asymmetric ceramic membranes are usually composed of alumina as the support layer and alumina, titania, or zirconia as the separation layer. The unique advantages of ceramic membranes over polymeric membranes are mostly ascribed to the intrinsic properties of ceramics such as their (1) excellent mechanical/chemical/thermal stability, (2) controlled pore size distribution and high porosity, and (3) good hydrophilicity [14, 15]. Therefore, ceramic membranes have been employed in an extensive range of applications across many industries.

One of the most critical issues in the development of effective membrane processes for water treatment is membrane fouling (particularly irreversible fouling) during filtration [16]. The mechanism of membrane fouling involves three key elements: (1) pore adsorption, (2) pore plugging, and (3) cake formation. Solutes with pore diameters similar to those of the membrane pores completely block them, whereas solutes of larger pore diameters form a cake layer on the surface of the membrane [17]. Consequently, membrane fouling causes a decrease in permeate flux and water quality, resulting in an increase in transmembrane pressure (TMP) and operational costs [18]. Thus, mitigating the adsorption (or deposition) of foulants on the membrane surface is essential for the development of ceramic membranes with superior fouling resistance. Numerous surface modification techniques have been reported for polymeric membranes [19]. In contrast, the surface modification of ceramic membranes has received less attention because of the limited modification methods available to date.

In our previous work, SiO_2 was surface-modified via a sol–gel process on a positively charged alumina support membrane to change the surface charge negatively at pH 6.5 [20]. Electrostatic repulsion thus occurred between the membrane surface and humic acid (HA) solution, and the flux performance of the modified membrane was much better than that of the pristine alumina membrane during membrane filtration, demonstrating the superiority of the SiO_2 surface modification.

Herein, we aimed to develop a unique functionality of ceramic membranes by achieving fouling resistance using SiO_2 and enhancing photocatalytic activity using TiO_2, which ultimately realizes the concept of self-cleaning ceramic membranes. Among the semiconductor catalysts, TiO_2 has received the highest interest in the development of photocatalysis technology. Due to low production cost and good chemical stability, this has been extensively employed in photocatalytic degradation of organic compounds (which contained nitrogen, hydrocarbons, and azo dyes) under a UV light source [21–23]. Nevertheless, considerable efforts have been made so as to overcome the restrictions of TiO_2 [i.e., large band gap (3.2 eV), and low quantum efficiency] and then facilitate the photocatalytic activity of TiO_2 even under visible light region [24–27]. The pristine alumina MF membranes were accordingly subjected to inorganic surface modification using a TiO_2/SiO_2 sol–gel process. The physicochemical properties of the TiO_2/SiO_2-coated MF membranes were analyzed in terms of surface morphology, crystalline structure, and pore size distribution. The fouling resistance and photocatalytic activity were further

investigated based on the time-dependent flux pattern and concentration reduction against a model foulant, respectively.

2 Experimental

2.1 Fabrication of alumina MF membranes

Alumina support layers were manufactured first using an α-alumina powder with a mean particle size of 4.8 μm (AM-210, Sumitomo Chemical Co. Ltd., Japan). Subsequently, the samples were sintered at 1600 °C for 1 h (heating rate of 5 °C/min). A normal coating procedure was adopted to prepare for alumina MF membranes using the above alumina support layers [28]. In brief, a table-top dip coater (E-flex, Republic of Korea) was utilized to produce an alumina separation layer on an alumina support layer. The coating slurry was composed of 10 wt% α-alumina with a mean particle size of 0.27 μm (AKP-30, Sumitomo Chemical Co. Ltd., Japan), polyvinyl alcohol (Junsei Chemical, Japan), glycerol (Sigma-Aldrich, USA), 2-propanol, ethyl alcohol, and deionized (DI) water. The alumina support layers were dip-coated for 10 s and subsequently withdrawn at a speed of 1 mm/s. The coated samples were dried under ambient conditions overnight and thereafter sintered at 1300 °C for 1 h at a heating rate of 3 °C/min.

2.2 Binary TiO_2/SiO_2 coating on alumina MF membranes

Tetraethyl orthosilicate (TEOS) and titanium isopropoxide (TIP) were used to introduce binary TiO_2/SiO_2 compositions on the alumina MF membranes to achieve unique surface characteristics. This is based on our previous research work, which revealed that inorganic surface modification with amorphous SiO_2 enhances the antifouling properties of pristine alumina support/MF membranes [20]. In the previous work, we solely focused on the improvement of antifouling properties through SiO_2 surface modification. However, in the present work, the binary TiO_2/SiO_2 compositions were introduced to achieve both antifouling properties and photocatalytic activity of the alumina MF membranes.

An ethanol/DI water mixture was prepared, and its pH was adjusted to 2.0 using 10 M HCl. TEOS was thereafter dissolved in the above mixture and stirred to obtain SiO_2 sol solutions. TiO_2 sol solutions prepared using TIP in ethanol were added drop-wise to the SiO_2 sol solution to produce binary TiO_2/SiO_2 compositions. After stirring for 30 min, the pristine alumina MF membranes were immersed in the binary TiO_2/SiO_2 sol solutions at room temperature. Subsequently, the membrane was washed with ethanol and dried in an oven. At the final stage, the TiO_2/SiO_2-coated membranes were calcinated at 500 °C for 6 h. The pristine alumina MF membranes were thus modified using an inorganic TiO_2/SiO_2 compound. The total molar concentration of the binary TiO_2/SiO_2 was fixed at 0.1 and the mole percentage of TiO_2 was controlled. These membranes were denoted as 80 mol% TiO_2, 50 mol% TiO_2, and 20 mol% TiO_2 according to the TiO_2 mole percentage in the binary TiO_2/SiO_2 compositions.

2.3 Characterization of TiO_2/SiO_2-coated alumina MF membranes

The physicochemical properties of alumina MF membranes subjected to surface modification and membrane fouling procedures were investigated. The surface morphology was analyzed using a field-emission scanning electron microscope (FE-SEM, JSM-6700F, JEOL, Japan) at magnifications of 1000× and 50,000× . The crystalline structure was analyzed by X-ray diffraction (XRD, D/Max 2500, Rigaku, Japan) using Cu kα radiation ($\lambda = 1.5406$ Å) at 40 kV and 200 mA. A scan range of 2θ is ranged from 10° to 80°. For XRD analysis, the powder types of TiO_2/SiO_2 were used by grinding the sol–gel processed TiO_2/SiO_2 samples after calcination at 500 °C. The pore size distributions of the membranes were characterized via mercury intrusion porosimetry (Autopore IV 9510, Micromeritics, USA). The specific surface area of the membranes was determined using the Brunauer–Emmett–Teller method (Autosorb-iQ, Quantachrome Instrument, USA).

2.4 Membrane permeation test of TiO_2/SiO_2-coated alumina MF membranes

The membrane permeation tests of TiO_2/SiO_2-coated MF membranes were carried out using a cross-flow microfiltration system (Lab-MPT, SepraTek Membrane System, Republic of Korea) [20, 29–31]. The feed solution was supplied at 25 °C using a circulating bath (JEIO TECH, Republic of Korea). The permeation tests were thereafter operated at a TMP of 2.0 bar with a fluid velocity of 2.5 L/min. The weight of the permeate was periodically measured using an electronic mass balance (CAS, Republic of Korea) for the calculation of flux data. The membrane fouling procedures made up of four steps. In step 1, the membranes were permeated using DI water for 30 min until a stable baseline flux was reached (J_0). In step 2, a model foulant (HA) was supplied to initiate membrane fouling for 1 h (J_p). The foulant solution was prepared with concentrations of 10 mg/L of HA (pH 6.5). In step 3, the fouled alumina membranes were allowed to back-washing for 10 min by a

10 mM sodium dodecyl sulfate solution (Sigma-Aldrich, USA) at pH 11. In step 4, DI water was introduced again for 30 min for a stable flux (J_1). These fouling processes were conducted in triplicate using three separate membranes, and their mean values were adopted for analysis. On the basis of the flux data obtained, antifouling properties such as flux decline ratio (%) and flux recovery ratio (%) were drawn using the following equations:

$$\text{Flux decline ratio}\,(\%) = \left(1 - \frac{J_p}{J_0}\right) \times 100, \quad (1)$$

$$\text{Flux recovery ratio}\,(\%) = \left(\frac{J_1}{J_0}\right) \times 100, \quad (2)$$

where J_0 is the DI water flux in step 1, J_p is the flux of the foulant solutions in step 2, and J_1 is the DI water flux in step 4.

As the additional characterization of the antifouling properties, the membrane permeation test was operated in circulation mode, i.e., HA solution (1 L) was added to the feed tank in step 2, and the permeate was sent back to the feed tank. The permeate (10 mL) in the feed tank was subsequently collected every 10 min. The concentrations of the foulants could thereafter be measured at 254 nm using ultraviolet–visible (UV–vis) spectroscopy (UV5, Mettler Toledo, USA). The membrane fouling ratio (%) was drawn using the following equation:

$$\text{Membrane fouling ratio}\,(\%) = \left(1 - \frac{C_p}{C_0}\right) \times 100, \quad (3)$$

where C_0 is the initial concentration of the foulants and C_p is the concentration of the permeates in step 2.

2.5 Photocatalytic degradation of TiO_2/SiO_2-coated alumina MF

For the analysis of photocatalytic degradation, the binary TiO_2/SiO_2-coated alumina MF membrane was submerged in darkness to cylindrical glass dish containing 50 mL of HA solution (10 mg/L) for 60 min so as to establish adsorption equilibrium. A UV lamp (365 nm, 15 W, VL-115, Vilber, France) was thereafter placed 5 cm above the HA solution and was ready to emit the UV light. The experiment for photocatalytic degradation began as soon as the UV lamp was turned on. In order to analyze the photocatalytic degradation ratio (%), 5 mL of the HA solution was collected every 30 min to measure UV absorbance at 254 nm using UV–vis spectroscopy (UV5, Mettler Toledo, USA). The photocatalytic degradation ratio (%) was calculated by a comparison between the initial HA concentration (C_0) and the HA concentrations at each designated time interval (C) using the following equation:

$$\text{Photocatalytic degradation ratio}\,(\%) = \left(1 - \frac{C}{C_0}\right) \times 100. \quad (4)$$

3 Results and discussion

3.1 Characterization of TiO_2/SiO_2-coated alumina MF membranes

In our previous research, alumina support membranes (pore size: 0.80 μm) were modified to form a SiO_2 coating layer via a sol–gel process [20]. Their physicochemical properties and membrane permeation were analyzed using a model foulant solution. Notably, the effectiveness of the newly formed SiO_2 layer was successfully demonstrated while retaining relatively higher flux values. For more advanced research work, we also endeavored to apply a SiO_2 sol–gel process to alumina MF membranes (instead of macroporous support membranes). The results of each characterization for SiO_2-coated MF membranes were demonstrated as well to illustrate the efficacy of SiO_2 coating to achieve antifouling properties [32].

Herein, TiO_2 was introduced to SiO_2 to impart not only fouling resistance but also photocatalytic activity to alumina MF membranes. The binary TiO_2/SiO_2 compositions were prepared via a sol–gel process with varied mole percentages of TiO_2 (80 mol% TiO_2, 50 mol% TiO_2, and 20 mol% TiO_2). It is thus expected that they will exhibit corresponding antifouling properties and photocatalytic activity depending on the TiO_2 contents.

The cross-sectional image of the pristine alumina MF membranes is shown in Fig. 1a, consisting of a support layer (made of coarse alumina particles) and separation layer (made of fine alumina particles). The top surface morphologies of the unmodified and TiO_2/SiO_2-coated alumina MF membranes were observed under a high magnification of 50,000× (Fig. 1b). The pristine alumina MF membrane appeared to have relatively larger pore volumes between the alumina particles than the TiO_2/SiO_2-coated MF membranes (80 mol% TiO_2, 50 mol% TiO_2, and 20 mol% TiO_2). With a decrease in the mole percentage of TiO_2, the pore volumes between the alumina particles appeared to reduce gradually, but it is difficult to distinguish them from the SEM images. In the case of 20 mol% TiO_2, the newly formed TiO_2/SiO_2 layer would likely fill the pore volumes to some extent, and consequently, pore blockage may occur. The binary TiO_2/SiO_2-coated MF membranes appear to be suitable for inorganic surface modification because the micro-pore reduction

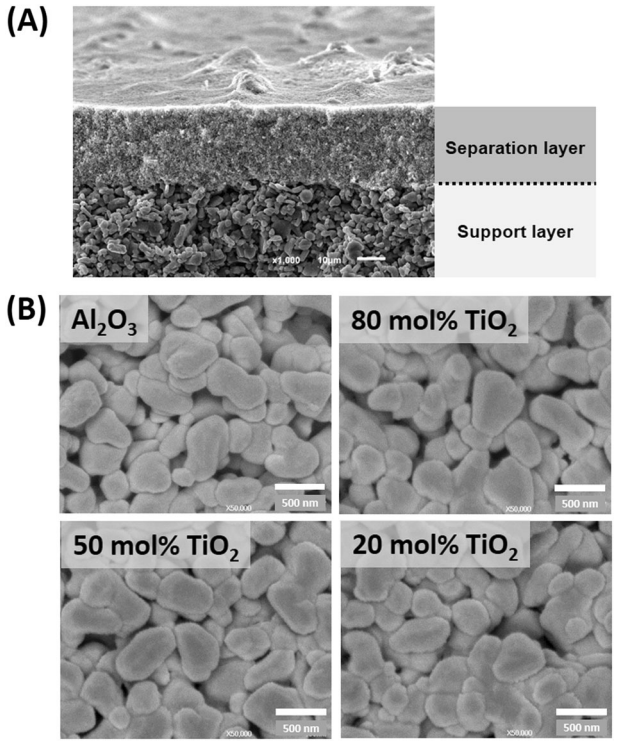

Fig. 1 SEM micrographs (cross-section) of **a** alumina-coated MF membrane consisting of a support layer and separation layer at a magnification of 1000×. **b** SEM micrographs (top surface) of the pristine and TiO_2/SiO_2-coated MF membranes at a magnification of 50,000×

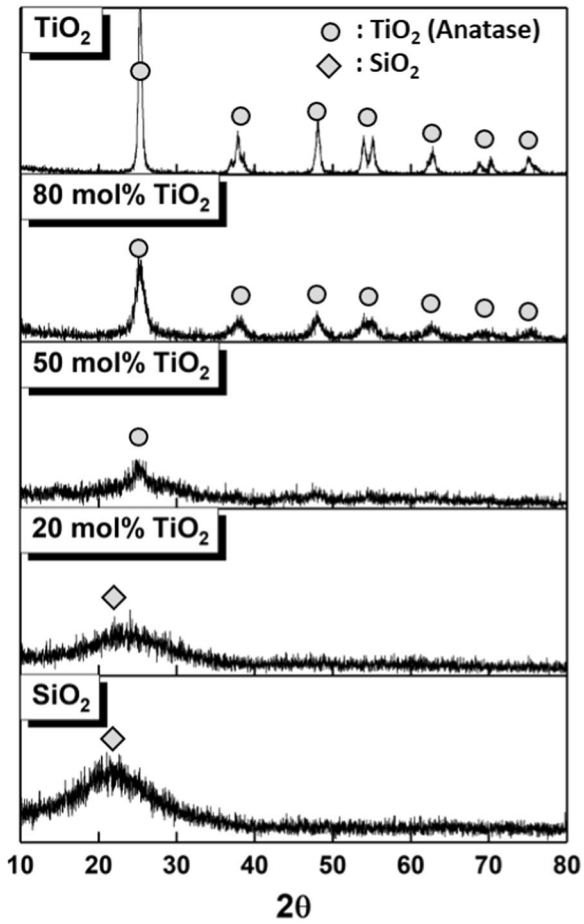

Fig. 2 XRD analysis of the binary TiO_2/SiO_2 compositions produced via sol–gel process (TiO_2, 80 mol% TiO_2, 50 mol% TiO_2, 20 mol% TiO_2, and SiO_2)

of alumina MF membrane is minimal. In our previous work, the SiO_2 coating on alumina support/MF membranes did not significantly alter membrane morphology as well, showing a minimal effect of inorganic surface modification [20]. In addition, the microscopic morphology of TiO_2/SiO_2-coated MF membranes was further examined using a transmittance electron microscope (TEM). More detailed images are displayed in Fig. 1S (Supplementary data). The TEM micrographs evidenced that the TiO_2/SiO_2 coating layers were allowed to form in a stable manner. This result well coincides with our previous research of stable formation of SiO_2 layers on alumina support membranes [20].

The XRD analysis of binary TiO_2/SiO_2 powders is carried out to demonstrate the stable formation of the TiO_2/SiO_2 layer (Fig. 2). The XRD patterns of pure TiO_2 and pure SiO_2 are provided for comparison. The characteristic peaks of TiO_2 (anatase) were detected at 2θ values of approximately 25°, 38°, 48°, 54°, 55°, 63°, 69°, and 75°. In contrast, the amorphous SiO_2 phase is broadly distributed near the 2θ value of 23°. The addition of SiO_2 to TiO_2 caused the phase transformation from TiO_2 (anatase) to amorphous SiO_2 incrementally. Samples with higher TiO_2 mole percentages (80 mol%) could retain the typical peaks of TiO_2 (anatase). However, they were likely to lose crystallinity gradually from 50 mol% to 20 mol% TiO_2. In the case of 20 mol% TiO_2, the patterns were almost identical to pure SiO_2 patterns. Similar to our result, the XRD analysis of binary TiO_2/SiO_2 compositions was also reported to indicate the gradual phase transformation from crystalline TiO_2 (anatase) to amorphous SiO_2 [33].

The pore size distributions of the alumina MF membranes were analyzed using mercury intrusion porosimetry to investigate the effect of the TiO_2/SiO_2 coating process (Fig. 3). Figure 3a, b shows two typical peaks for the separation and support layers and similar pore size distribution patterns. The average pore sizes of the pristine MF membrane were determined to be 0.83 μm (support layer) and 0.124 μm (separation layer). In other words, it is evident that the support layer (having a coarse pore structure at the bottom) and the separation layer (having a dense pore structure at the top) are well aligned. Owing to the TiO_2/SiO_2 coating on the membrane surface, the pore sizes of inorganic surface-modified membranes gradually decreased depending on the TiO_2 mole percentages. In the separation region (Fig. 3a), the average pore sizes of the TiO_2/SiO_2-coated membranes were observed to decrease in the following order: 0.124 μm

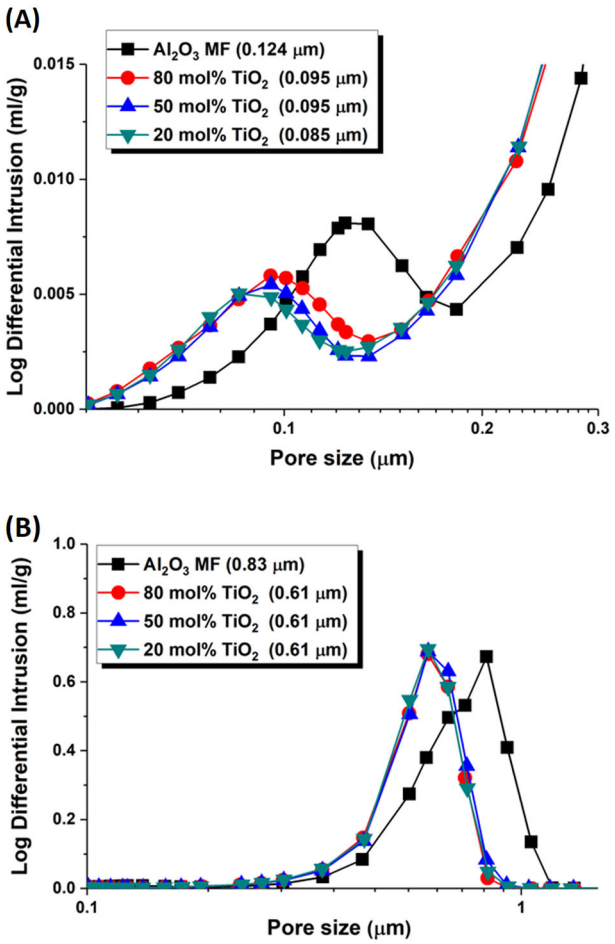

Fig. 3 Effect of binary TiO_2/SiO_2-coating on the pore size distribution of alumina MF membranes. The representative peaks for **a** separation and **b** support layers were measured

(pristine) > 0.095 μm (80 mol% TiO_2) ≥ 0.095 μm (50 mol% TiO_2) > 0.085 μm (20 mol% TiO_2). However, the pore size pattern in the support region is slightly different from that in the separation region. Owing to the formation of the new TiO_2/SiO_2 layers, the average pore size of the pristine alumina MF membranes decreased from 0.83 to 0.61 μm, irrespective of the mole percentage of TiO_2. The TiO_2/SiO_2 coating layers caused gradual pore size variations of the micro-pores in the separation region, but resulted in uniformly reduced pore sizes in the micro-pores of the support region. This led to a quantitative analysis of the reduction in micro-pore size owing to inorganic surface modification. In the support region, the pore size of 0.22 μm was diminished by TiO_2/SiO_2 coating process whereas the pore size reduction of 0.039 μm was observed in the separation region. It is expected that there will be no significant loss of pure water permeability because the pore size reduction in the separation region, which has a significant influence on the water permeation, is relatively small. Similarly, the newly formed SiO_2 layer on the alumina support/MF membranes would

Table 1 Specific surface areas (m^2/g) of binary TiO_2/SiO_2-coated alumina MF membranes

BET	Pristine Al_2O_3	80 mol% TiO_2	50 mol% TiO_2	20 mol% TiO_2
Specific surface area (m^2/g)	2.39	1.99	1.90	1.84

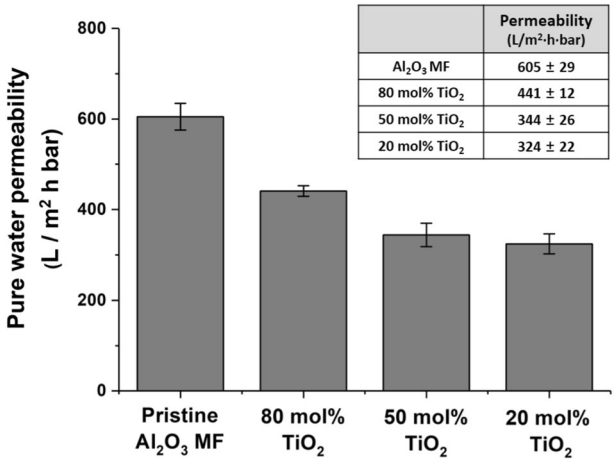

Fig. 4 Pure water permeability ($L/(m^2\,h\,bar)$) of the binary TiO_2/SiO_2-coated MF membranes. Detailed information on permeability is presented in the inset

reduce the pore sizes during the inorganic surface modification. Furthermore, the smaller pore sizes could result in a slight decrease in the pure water permeability [20].

The specific surface area (m^2/g) of the binary TiO_2/SiO_2-coated alumina MF membranes is given in Table 1. The pristine alumina MF membranes possessed the largest specific surface area (2.39 m^2/g), and it varied as follows according to the TiO_2 mole percentage; 80 mol% TiO_2 (1.99 m^2/g) > 50 mol% TiO_2 (1.90 m^2/g) > 20 mol% TiO_2 (1.84 m^2/g). This result (Table 1) is closely correlated with the pore size distribution in the separation layer (Fig. 3a). The smaller the pore sizes in the separation layer (which are attributed to the formation of TiO_2/SiO_2 layer), the less is the specific surface area with a decrease in TiO_2 content. It can be explained that the reduction of available pore volumes reduced the specific surface area owing to the formation of the TiO_2/SiO_2 coating layers.

The water permeability of inorganic surface-modified membranes has been considered a major parameter for estimating membrane productivity and efficiency. Thus, the pure water permeability of the TiO_2/SiO_2-coated alumina MF membranes was examined and the results are presented in Fig. 4. The pristine alumina MF membrane showed the highest pure water permeability of 605 ± 29 $L/(m^2\,h\,bar)$. However, as the pore size (especially in the separation region) decreased owing to inorganic surface modification,

the pure water permeability gradually declined. In the case of 80 mol% TiO_2, the pure water permeability was maintained at 441 ± 12 L/(m^2 h bar). When the TiO_2 contents reached 50 mol% and 20 mol%, the pure water permeability decreased to 344 ± 26 L/(m^2 h bar) and 324 ± 22 L/(m^2 h bar), respectively. The analysis of the above results (Fig. 4) in relation to the pore size results (Fig. 3) confirms that there is a close correlation between the micro-pore size in the separation region and the pure water permeability. The lowest water permeability (324 ± 22 L/(m^2 h bar)) was demonstrated in 20 mol% TiO_2 having the smallest average pore size (0.085 μm). Conversely, the pristine alumina MF membranes without any modification exhibited the largest pore size (0.124 μm) and the highest pure water permeability (605 ± 29 L/(m^2 h bar)).

Previous studies on organic surface modification have also observed a correlation between the pore size and pure water permeability of the alumina MF membranes [31]. It is normally accepted that an increase in the degree of surface grafting (or coating) would narrow down the pore size, surface roughness, and water permeability. In spite of the predominant features of inorganic surface modification, this commonly leads to a decline in the flux owing to the "pore-filling" effect [34].

In this work, TiO_2/SiO_2 coating on alumina MF membranes did not significantly alter either the physical properties of the membrane or the water permeability. Moreover, some membrane properties, such as pore size distribution and water permeability, could be varied by regulating the TiO_2 mole percentages. It is thus important to determine the optimum TiO_2/SiO_2 coating that would develop both fouling resistance and photocatalytic degradation while minimizing variations in the surface morphology, pore size, and water permeability

3.2 Antifouling and photocatalytic features of TiO_2/SiO_2-coated alumina MF membranes

We have previously confirmed that the fouling resistance of ceramic MF membranes is significantly encouraged by a SiO_2 sol–gel coating against model foulants [20]. This is mostly attributed to the strong electrostatic repulsion forces generated between the SiO_2-coated ceramic MF membranes and negatively charge model foulants, such as HA and bovine serum albumin. Based on these findings, the aim of this work is to create new functionality beyond the simple separation process of ceramic membranes for water purification. We are interested in simultaneously achieving antifouling properties and photocatalytic activity in order to enhance the functionality of ceramic membranes. The separation layer determines the separation performance of ceramic MF/UF membranes. It is extremely susceptible to membrane fouling because various foulants (or suspended particles) are mostly filtered out at this layer. Therefore, if the photocatalytic activity is established by regulating the coating materials existing in the separation layer, the separation of foulants (or suspended particles) and the decomposition of organic compounds causing membrane fouling can be carried out simultaneously. This is expected to contribute significantly to the realization of self-cleaning ceramic membranes while extending the membrane cleaning cycle and accelerating productivity. TiO_2 has been known to have self-cleaning properties owing to two photo-induced phenomena: photocatalysis and superhydrophilicity [35]. The photocatalysis can decompose organic foulants under ultraviolet light, which can be applied in air and water purification systems [32]. The photo-induced superhydrophilicity can readily wash off foulants (or suspended particles) from the surfaces (or pores), which imparts anti-fogging and easy cleaning properties [36]. Herein, we endeavored to develop a binary TiO_2/SiO_2 coating technique that can achieve both fouling resistance of SiO_2 and photocatalytic activity of TiO_2 using the mixture of SiO_2 and TiO_2 precursors. Hydrophobic HA (IEP: 4.7) was selected as a model foulant to simulate soluble humic substances that are ubiquitous in secondary treated effluents. The membrane fouling pattern would possibly be different from TiO_2/SiO_2-coated MF membranes, depending on TiO_2 mole percentages. As the amount of SiO_2 increases, the fouling resistance is likely to be improved. Conversely, when the amount of TiO_2 increases, the photocatalytic activity is anticipated to accelerate.

The normalized time-dependent flux pattern of the TiO_2/SiO_2-coated MF membranes is shown in Fig. 5 (step 1: DI water, step 2: HA solution, step 3: back-washing, and step 4: DI water). The membrane permeation tests were performed three times for each MF membrane to acquire reliable outcomes. All the MF membranes retained a stable flux

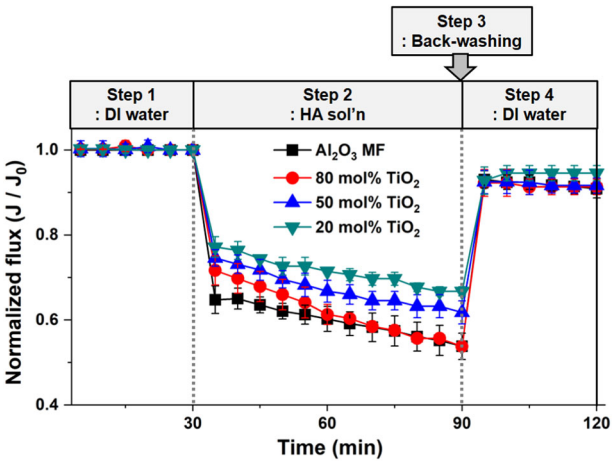

Fig. 5 Normalized flux patterns of binary TiO_2/SiO_2-coated MF membranes with HA solution (10 mg/L, pH 6.5)

Table 2 Membrane filtration performance of binary TiO_2/SiO_2-coated alumina membranes using HA (10 mg/L) solutions throughout the membrane fouling processes (step 1 to step 4)

HA solution	Flux decline ratio (%)	Flux recovery ratio (%)
Al_2O_3 MF	46 ± 3	91 ± 2
80 mol% TiO_2	46 ± 0	91 ± 2
50 mol% TiO_2	38 ± 3	92 ± 2
20 mol% TiO_2	33 ± 1	95 ± 2

The flux decline ratio (%) and flux recovery ratio (%) were calculated using the equation given in Section 2.4

level at step 1. As the HA solution was added in step 2 (Fig. 5), a very rapid flux decline occurred for each MF membrane, followed by a slower decrease with the increase in time. The flux level descended in the order of 20 mol% TiO_2 > 50 mol% TiO_2 > 80 mol% TiO_2 > pristine MF membrane, whereas the flux decline ratio (%) ascended in the order of 20 mol% TiO_2 < 50 mol% TiO_2 < 80 mol% TiO_2 < pristine MF membrane (Table 2). Samples with the highest TiO_2 content (80 mol% TiO_2) had lower flux values (or higher flux decline ratios) than samples with lower TiO_2 content (20 mol% and 50 mol% TiO_2), whereas samples with the lowest TiO_2 content (20 mol% TiO_2) exhibited the greatest flux performance. Although the samples (20 mol% TiO_2) have a smaller pore size and lower water permeability, outstanding fouling resistance is accomplished against HA solution. This is mainly ascribed to the higher SiO_2 content and the reduced effect of pore size restriction. In step 4, DI water was fed again after back-washing for 10 min, and thus, the flux recovery ratios (%) can be estimated (Table 2). Most of the MF membranes exhibited excellent flux recovery ratios (91–95%). Among them, samples with the lowest TiO_2 content (20 mol% TiO_2) presented the greatest flux recovery ratio (%) (95%). This indicated that the dominant cause of membrane fouling was reversible fouling rather than irreversible fouling. In other words, the flux loss (%) owing to irreversible fouling can be observed as approximately 5–9%.

As another standard to estimate antifouling properties, the membrane fouling ratios (%) of TiO_2/SiO_2-coated MF membranes were analyzed and the results are shown in Fig. 6. All MF membranes were severely fouled by HA solution at the initial stage of permeation before reaching steady levels (Fig. 6). The pristine alumina MF membranes presented the largest membrane fouling ratio (99%), and other TiO_2/SiO_2-coated MF membranes followed in the order of 80 mol% TiO_2 (98%), 50 mol% TiO_2 (97%), and 20 mol% TiO_2 (95%) with slight differences. The lower the content of TiO_2 in the coating layers, the more gradually the membrane fouling ratio (%) diminished.

The fouling resistance of ceramic membranes can be evaluated with respect to membrane permeation pattern

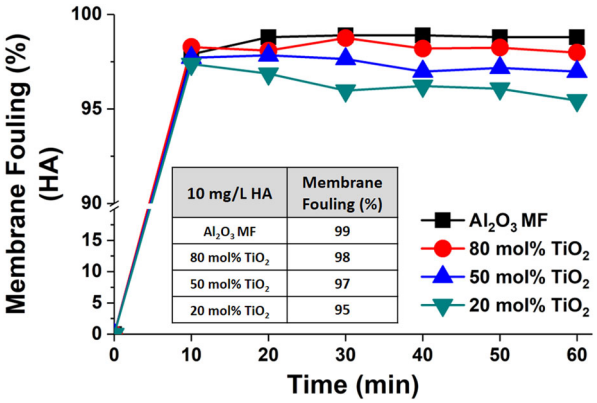

Fig. 6 Membrane fouling ratio (%) of the binary TiO_2/SiO_2-coated MF membranes. Membrane filtration was performed in circulation mode (step 2) using HA solution (10 mg/L, pH 6.5), and the concentrations in bulk and permeate were detected for calculation

(Fig. 5) and membrane fouling ratio (Fig. 6) by adopting HA solution as a model foulant. It is reported that the HA solution contained a wide molecular weight distribution (approximately 10 kDa to 0.45 μm) [37]. Especially, the components exceeding a size of 0.1 μm was almost 8%. These large-molecular-weight components, whose sizes were close to or larger than the membrane pore sizes, led to pore blockage and cake formation [38]. This would cause a rapid flux decline in the early stage followed by a more gradual decrease (Fig. 5).

The SEM morphology for the fouled and back-washed MF membranes is exhibited in Fig. 7. The early MF membranes were seriously fouled by the HA solution. However, they were mostly recovered throughout back-washing. The gross images are also provided to observe the noticeable fouling resistance of the TiO_2/SiO_2-coated MF membranes. The pristine MF membrane became dark brown in step 2, which was mostly attributed to the excessive HA fouling. In contrast, the fouling behavior of TiO_2/SiO_2-coated MF membranes varied in color depending on the TiO_2 content. Samples with the least TiO_2 content (20 mol% TiO_2) exhibited the lowest fouling, followed by samples with ascending TiO_2 content (50 mol% and 80 mol% TiO_2). Nevertheless, samples with the highest TiO_2 content (80 mol% TiO_2) demonstrated much higher fouling resistance than the pristine alumina MF membrane. The excellent consistency of the membrane fouling patterns (Fig. 5) with the corresponding SEM images (Fig. 7) is distinctly illustrated. Higher flux behaviors and better fouling resistance were observed with a decrease in TiO_2 mole percentage despite the narrow pore size distribution of the TiO_2/SiO_2-coated MF membranes. Accordingly, there are optimum compositions of the binary TiO_2/SiO_2 that can not only retain the unique micro-porous structures but also contribute to the antifouling properties.

The photocatalytic degradation of TiO_2/SiO_2-coated alumina MF membranes was analyzed using the HA

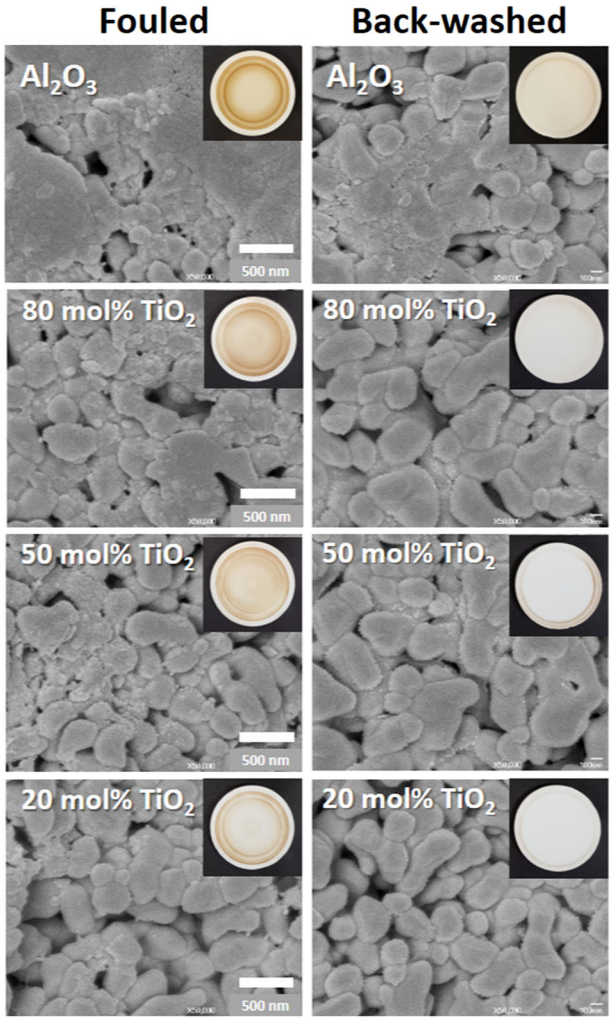

Fig. 7 SEM micrographs of binary TiO_2/SiO_2-coated MF membranes subjected to fouling procedures using HA solution (10 mg/L, pH 6.5). For SEM analysis, specimens were observed at a magnification of 50,000×. Gross images were provided for HA-fouled MF membrane, which led to the brown staining

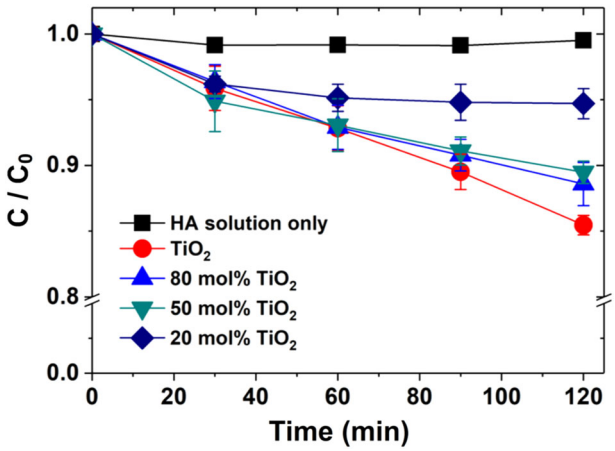

Fig. 8 Photocatalytic degradation of binary TiO_2/SiO_2-coated alumina MF membranes. HA solution (10 mg/L, pH 6.5) was provided to simulate the actual water environment for the development of the photocatalytic activity of ceramic membranes

solution (Fig. 8). Many research works on photocatalysis have utilized dyeing reagents such as methylene blue and methyl orange as model foulants [39–41]. However, herein, the HA solution was introduced to simulate the actual water environment for the development of the photocatalytic activity of ceramic membranes. Prior to beginning the photocatalytic degradation test, the binary TiO_2/SiO_2-coated alumina MF membranes were submerged in HA solution for 60 min so as to establish adsorption equilibrium. This procedure could exclude the adverse effect of HA adsorption on the experimental errors which might cause the abnormal increase of photocatalytic degradation ratio (%). Regarding HA adsorption to ceramic membranes, we additionally measured the HA adsorption ratio (%) after reaching adsorption equilibrium (for 60 min). The adsorption ratio (%) of HA was calculated as 0.4–0.6% throughout all membranes. As a result, it indicated that the adsorption ratio (%) of HA to TiO_2/SiO_2-coated alumina MF membranes was very negligible.

Pure TiO_2-coated samples and HA solution only were adopted as the positive and negative controls, respectively, which revealed the corresponding photocatalytic degradation ratios of 14.5% and 0.5% at 120 min. As shown in Fig. 8, samples with higher TiO_2 content (50 mol% and 80 mol%) exhibited almost the same photocatalytic degradation ratio (%) as pure TiO_2 at 60 min, but they began to show a gradual decrease in the photocatalytic degradation ratio compared with that of pure TiO_2 at 90 and 120 min. At 120 min, the photocatalytic degradation ratio (%) descended in the order of pure TiO_2 (14.5%) > 80 mol% TiO_2 (11.4%) > 50 mol% TiO_2 (10.5%) > 20 mol% TiO_2 (5.3%) > HA solution only (0.5%). In particular, samples with 50 mol% TiO_2 exhibited a photocatalytic degradation ratio (%) similar to that of samples with 80 mol% TiO_2, even though the TiO_2 content was half of the total 0.1 M of the TiO_2/SiO_2 compositions. Moreover, they achieved superior fouling resistance with the second largest flux performance after that of samples with 20 mol% TiO_2. Therefore, the surface modification of alumina MF membranes with 0.1 M TiO_2/SiO_2 (especially 50 mol% TiO_2) could achieve both fouling resistance and photocatalytic activity via a TiO_2/SiO_2 sol–gel process.

In this work, the total concentration of the binary TiO_2/SiO_2 was fixed at 0.1 M because this was the optimum coating conditions for ceramic MF membranes with respect to surface morphology and pore size distribution. On the one hand, it was feasible to increase the total binary concentration and TiO_2 mole percentage, so that the noticeable improvement of the photocatalytic activity could be expected. But, on the other hand, it could be difficult to carry out the normal MF

membrane performance test because the unique microstructure of ceramic MF membranes would be severely eliminated due to the high concentration of TiO_2/SiO_2. Based on our previous research work, it was found that if the total concentration reached at 0.2 M, the top surface of ceramic MF membranes would be completely wrapped with the coating layer and the microporous structure cannot be observed [42].

4 Conclusions

Noticeable fouling resistance and photocatalytic degradation of the TiO_2/SiO_2-coated alumina MF membranes were obtained using HA solution as a model foulant. This investigation is an extension of our previous work, in which SiO_2 sol–gel coating was carried out on alumina support/MF membranes to achieve superior fouling resistance. Herein, we fostered new inorganic surface modification techniques not only for enhancing fouling resistance but also for imparting photocatalytic activity. The efficacy of TiO_2/SiO_2 coating on alumina MF membranes was successfully demonstrated for samples with 50 mol% TiO_2, which exhibited both the second highest flux performance and greater photocatalytic degradation ratio (%).

Acknowledgements This work was supported by the Technology Innovation Program (10053611) funded by the Ministry of Trade, Industry & Energy (MI, Republic of Korea) and the Fundamental Research Program (PNK6340) in Korea Institute of Materials Science (KIMS).

Compliance with ethical standards

Conflict of interest The authors declare that they have no conflict of interest.

References

1. Kumar SM, Madhu G, Roy S (2007) Sep Purif Technol 57:25
2. Kim J, Van der Bruggen B (2010) Environ Pollut 158:2335. https://doi.org/10.1016/j.envpol.2010.03.024
3. Krstić DM, Antov MG, Peričin DM, Höflinger W, Tekić MN (2007) Biochem Eng J 33:10. https://doi.org/10.1016/j.bej.2006.08.016
4. Finley J (2005) Filtr Sep 42:34
5. Majewska-Nowak KM (2010) Desalination 254:185
6. Suresh K, Pugazhenthi G (2014) Desalin Water Treat 57:1927. https://doi.org/10.1080/19443994.2014.979445
7. DeFriend KA, Wiesner MR, Barron AR (2003) J Membr Sci 224:11
8. Benito J, Conesa A, Rubio F, Rodriguez M (2005) J Eur Ceram Soc 25:1895
9. Van Gestel T, Sebold D, Kruidhof H, Bouwmeester HJ (2008) J Membr Sci 318:413
10. Zhou M, Roualdès S, Ayral A (2015) Eur Phys J Spec Top 224:1871
11. Nwogu NC, Kajama M, Gobina E (2015) Compos Struct 134:1044
12. Fukushima M, Zhou Y, Yoshizawa Y-i (2009) J Membr Sci 339:78
13. Maghsoudi H (2016) Sep Purif Rev 45:169
14. Verweij H (2003) J Mater Sci 38:4677
15. Cot L, Ayral A, Durand J et al. (2000) Solid State Sci 2:313
16. Shannon MA, Bohn PW, Elimelech M, Georgiadis JG, Marinas BJ, Mayes AM (2008) Nature 452:301. https://doi.org/10.1038/nature06599
17. Vu A, Darvishmanesh S, Marroquin M, Husson SM, Wickramasinghe SR (2016) Sep Sci Technol 51:1370. https://doi.org/10.1080/01496395.2016.1150295
18. Madaeni SS, Mohamamdi T, Moghadam MK (2001) Desalination 134:77
19. Rana D, Matsuura T (2010) Chem Rev 110:2448
20. Wang F, Lee J, Ha J-H, Song I-H (2017) Mater Lett 191:200
21. Klare M, Scheen J, Vogelsang K, Jacobs H, Broekaert JAC (2000) Chemosphere 41:353. https://doi.org/10.1016/S0045-6535(99)00447-6
22. Cermenati L, Dondi D, Fagnoni M, Albini A (2003) Tetrahedron 59:6409. https://doi.org/10.1016/S0040-4020(03)01092-5
23. Alaton IA, Balcioglu IA (2001) J Photochem Photobiol 141:247. https://doi.org/10.1016/S1010-6030(01)00440-3
24. Ong CB, Ng LY, Mohammad AW (2018) Renew Sustain Energy Rev 81:536. https://doi.org/10.1016/j.rser.2017.08.020
25. Ishimaki K, Uchiyama T, Okazaki M, Lu D, Uchimoto Y, Maeda K (2018) Bull Chem Soc Jpn 91:486. https://doi.org/10.1246/bcsj.20170373
26. Su T, Shao Q, Qin Z, Guo Z, Wu Z (2018) ACS Catal 8:2253. https://doi.org/10.1021/acscatal.7b03437
27. Li H, Li J, Ai Z, Jia F, Zhang L (2018) Angew Chem Int Ed Engl 57:122. https://doi.org/10.1002/anie.201705628
28. Ha J-H, Bukhari SZA, Lee J, Song I-H, Park C (2016) Ceram Int 42:13796
29. Lee J, Ha J-H, Song I-H (2016) Sep Sci Technol 51:2420
30. Lee J, Ha J-H, Song I-H (2017) Desalination Water Treat 88:16
31. Lee J, Ha J-H, Song I-H, Shin DW (2017) J Ceram Soc Jpn 125:899
32. Fujishima A, Zhang X, Tryk DA (2008) Surf Sci Rep 63:515
33. Erdural B, Bolukbasi U, Karakas G (2014) J Photochem Photobiol 283:29. https://doi.org/10.1016/j.jphotochem.2014.03.016
34. Wang P, Meng J, Xu M et al. (2015) J Membr Sci 492:547. https://doi.org/10.1016/j.memsci.2015.06.024
35. Guan K (2005) Surf Coat Technol 191:155
36. Wang R, Hashimoto K, Fujishima A et al. (1997) Nature 388:431
37. Hashino M, Hirami K, Katagiri T et al. (2011) J Membr Sci 379:233. https://doi.org/10.1016/j.memsci.2011.05.068
38. Yuan W, Zydney AL (1999) J Membr Sci 157:1. https://doi.org/10.1016/S0376-7388(98)00329-9
39. Athanasekou CP, Moustakas NG, Morales-Torres S et al (2015) Appl Catal B: Environ 178:12. https://doi.org/10.1016/j.apcatb.2014.11.021
40. Momeni M, Saghafian H, Golestani-Fard F, Barati N, Khanahmadi A (2017) Appl Surf Sci 392:80. https://doi.org/10.1016/j.apsusc.2016.08.165
41. Zhang G, Song A, Duan Y, Zheng S (2018) Microporous Mesoporous Mater 255:61. https://doi.org/10.1016/j.micromeso.2017.07.028
42. Lee J, Ha J-H, Song I-H, Park J-W (2019) J Ceram Soc Jpn 127:35. https://doi.org/10.2109/jcersj2.18124